High Spectral Efficiency 400 Gb/s Transmission by Different Modulation Formats and Advanced DSP

Miao Kong, Xinying Li, Jiao Zhang, Kaihui Wang, Xiangjun Xin, Feng Zhao, and Jianjun Yu, *Senior Member, IEEE, Fellow, OSA*

***Abstract*—We experimentally demonstrate probabilistically shaped 64-ary quadrature-amplitude-modulation (64QAM) 50-GHz-grid wavelength-division-multiplexing (WDM) transmission with a bit rate of 400-Gbit/s per channel over 3,600-km Raman-amplified ultra-large effective area fiber (ULAF). Our results show that the probabilistically shaped 64QAM outperforms the hybrid-32/64QAM by 50% reach improvement. Thanks to pre-equalization and look-up-table pre-distortion, a 5.5-dB optical signal-to-noise ratio (OSNR) gain can be obtained. Furthermore, utilizing ULAF with Raman amplifier causes an apparent improvement on the transmission performance compared with using the SSMF with EDFA. We also compare the optical coupler with the wavelength selective switch utilized in the WDM system to explore a suitable way for WDM transmission. Advanced DSP including Butterworth low-pass digital filter is also used at the receiver end.**

***Index Terms*—Hybrid quadrature-amplitude-modulation (hybrid-QAM), look-up-table (LUT) pre-distortion, optical coupler, pre-equalization, probabilistic shaping, ultra large effective area fiber (ULAF).**

I. Introduction

With the rapid growth of Internet bandwidth demand, 400G wavelength division multiplexing (WDM) transmission has become a hotspot of research in the last few years [1]–[5]. In order to realize the required 400G bit-rate per channel, higher-level modulation formats, such as 64-ary quadrature-amplitude-modulation (64QAM), can be a good candidate for 400G WDM transmission based on the 50-GHz grid with high spectral efficiency. The soft-decision forward error correction (SD-FEC) threshold with 30.9% overhead requires a 44-Gbaud rate for a regular-64QAM. However, higher-level modulation formats require higher optical signal-to-noise ratio (OSNR), which means that the transmission distance will be limited. In other words, the regular-64QAM modulation is not an optimal modulation format for 400G WDM that is required to meet the demands of both higher bit-rate and longer reach distance. Compared with regular-64QAM, regular-32QAM can settle the OSNR requirements, however, the required baud-rate for regular-32QAM, which is above 52G, is not available for 50-GHz WDM. Recently, hybrid-QAM [6], [7] and probabilistic shaping (PS) technique [8]–[14] have been demonstrated to yield OSNR sensitivity gain and transmission distance improvement. Different from regular-QAM, hybrid-QAM, which consists of two or more regular-QAMs with different source entropies that are time-interleaved at various ratios within a frame, can realize any entropy that falls between the entropies of the two regular-QAMs. In this way, the gap between regular-32QAM and regular-64QAM can be filled smoothly by hybrid-32/64QAM, which can yield a better compromise between spectral efficiency and OSNR sensitivity compared with regular-32QAM and regular-64QAM. Undoubtedly, hybrid-32/64QAM signals can obtain a better OSNR sensitivity when the entropy is closer to the regular-32QAM with better tolerance for OSNR. However, lower entropy means a higher baud-rate, which may cause more crosstalk from adjacent WDM channels. Thus, choosing an optimal hybrid ratio (entropy) for hybrid-32/64QAM can be significant. As for the PS technique, a power-efficient Maxwell-Boltzmann distribution is used in order to decrease the gap between the capacity of communication systems and the Shannon limit [11]–[26]. It is therefore interesting to compare hybrid-QAM with PS technology to explore a better modulation format for 400G WDM transmission based on the 50-GHz grid.

Moreover, a new ultra-large effective area fiber (ULAF) with Raman amplification can be adopted to effectively extend the transmission distance compared with the standard single-mode fiber (SSMF) with Erbium-doped fiber amplifier (EDFA) [15]. In addition, normalized generalized mutual information (NGMI) has been reported to be a reliable FEC threshold for both regular-QAM and PS-QAM modulation formats [16]. Particularly, the approximate NGMI values, which will be proved to be a reasonable SD-FEC threshold with 27.5% and 30.9% overheads in Section II, are 0.8 and 0.784, respectively.

In this paper, we compare hybrid-QAM modulation formats with different hybrid methods and hybrid ratios to select an optimal hybrid-QAM format and entropy, that is hybrid-32/64QAM with an entropy of 5.5 bit/symbol/polarization. We

Manuscript received June 3, 2019; accepted July 28, 2019. Date of publication August 1, 2019; date of current version September 30, 2019. This work was supported in part by the National Key Research and Development Program of China (No. 2018YFB1800905) and in part by NNSF of China (No. 61527801, 61675048, 61720106015, 61835002, and 61805043). *(Corresponding author: Jianjun Yu.)*

M. Kong, X. Li, J. Zhang, K. Wang, and J. Yu are with the Department of Communication Science and Engineering, and Key Laboratory for Information Science of Electromagnetic Waves (MoE), Fudan University, Shanghai 200433, China (e-mail: 17110720016@fudan.edu.cn; smileseaxy@gmail.com; 17110720046@fudan.edu.cn; 16110720021@fudan.edu.cn; jianjun@fudan.edu.cn).

X. Xin is with Beijing University of Posts and Telecommunications, Beijing 100191, China (e-mail: xjxin@bupt.edu.cn).

F. Zhao is with Xi'an University of Posts and Telecommunications, Xi'an 710121, China (e-mail: hfengzhao@xupt.edu.cn).

Color versions of one or more of the figures in this paper are available online at http://ieeexplore.ieee.org.

Digital Object Identifier 10.1109/JLT.2019.2932384

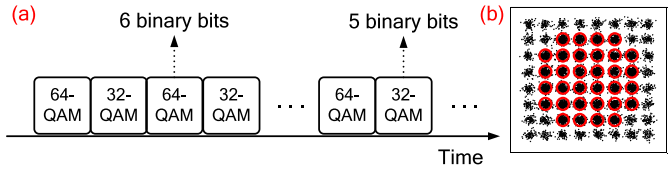

Fig. 1. (a) Symbol mapping and (b) constellation of a time-domain hybrid-32/64QAM with an entropy of 5.5-bit/symbol/polarization.

also compare the optical coupler (OC) with the wavelength selective switch (WSS) to explore a more efficient format for implementing WDM. We experimentally demonstrate an eight-channel WDM transmission on the 50-GHz grid over Raman-amplified ULAF, using polarization multiplexing (PM) PS-64QAM and hybrid-32/64QAM modulation, respectively. Both PS-64QAM and hybrid-32/64QAM signals have an entropy of 5.5 bit/symbol/polarization. ULAF with Raman amplification is utilized to further improve the reach distance. Using the DSP-based pre-processing, namely pre-equalization and look-up-table (LUT) pre-distortion [18]–[25], we realize the 8×48-Gbaud (8×528-Gbit/s line rate and 8×403-Gbit/s net bit rate) WDM transmission over 3,600-km ULAF with Raman amplification based on PS-64QAM considering the 27.5% SD-FEC threshold of 0.8 NGMI. Furthermore, we experimentally compare PS-64QAM with hybrid-32/64QAM at the same bit rate and the results show that PS-64QAM outperforms hybrid-32/64QAM by 50% transmission distance improvement in the 400G 50-GHz WDM system.

II. Principle of Hybrid-32/64QAM and PS-64QAM

As we know, regular 2^n-ary QAM can only realize integer entropy, while a recently proposed hybrid-QAM can achieve arbitrary entropy by assigning different time slots to two or more regular 2^n-ary QAMs with different entropies and fill the gap between regular-QAMs smoothly. To take the hybrid-32/64QAM with a hybrid ratio of 1:1 (with an entropy of 5.5-bit/symbol/polarization) as an example, regular-32QAM symbols (mapped to 5 bits) and regular-64QAM symbols (mapped to 6 bits) appear in turns following the ratio of 1:1, as shown in Fig. 1-(a). The corresponding constellation is illustrated in Fig. 1-(b).

Different from hybrid-QAM, PS uses a power-efficient Maxwell-Boltzmann distribution shown in equation (1) to increase the probability of constellation points with smaller amplitude but decrease the probability of constellation points with larger amplitude and therefore it can realize a lower average power at the same entropy and obtain a shaping gain.

$$P_X(x_i) = \frac{\exp(-v(\mathrm{Re}(x_i)^2 + \mathrm{Im}(x_i)^2))}{\sum_{k=1}^{M} \exp(-v(\mathrm{Re}(x_k)^2 + \mathrm{Im}(x_k)^2))} \quad (1)$$

Where x_i denotes the i-th complex M-QAM constellation point and v denotes the shaping parameter. Moreover, hybrid-QAM is made up of different regular-QAMs and its components maintain their individual numbers of mapped bits per symbol, while PS technique realizes the designated probability distribution of symbols by introducing redundancy and therefore the original number of mapped bits per symbol is maintained.

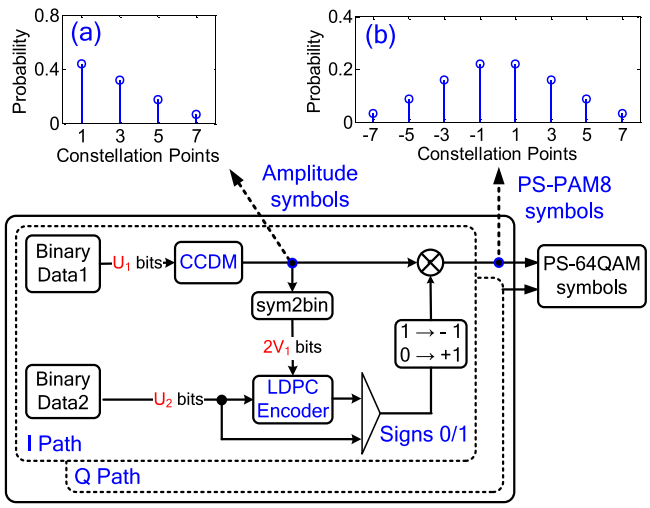

Fig. 2. Principle of PAS transmitter system.

It is universally acknowledged that PS is an excellent technology to achieve rates close to Shannon's limit and probabilistic amplitude shaping (PAS) [9], [12] has become a standard scheme, which carries out shaping by a distribution matcher (DM) before FEC encoding. The principle of combining DM with FEC encoder based on PS-64QAM with an entropy of 5.5-bit/symbol/polarization is shown in Fig. 2. Firstly, the binary data source is split into two parts consisting of $U_1 = 56678$ and $U_2 = 11435$ bits, respectively. U_1 bits are fed into a constant composition distribution matcher (CCDM) and $V_1 = 32400$ amplitude symbols {1, 3, 5, 7} are generated according to the designated probability distribution. Inset (a) of Fig. 2 offers the probability distribution of amplitude symbols generated by CCDM. Then the amplitude symbols are mapped into $2V_1$ binary bits, and these mapped bits are fed together with the U_2 bits into a low-density parity-check coded (LDPC) encoder with 27.5% overhead, which generates parity bits. These parity bits together with the U_2 bits, which both follow uniform distribution, are used as sign bits according to the mapping ($0 \rightarrow +1$ and $1 \rightarrow -1$). These mapped signs are then combined with the previous amplitude symbols to form $\{+1, +3, +5, +7\}$ or $\{-1, -3, -5, -7\}$ symbols, which are just the generated PS-PAM8 symbols as shown in inset (b) of Fig. 2. At last, two paths of PS-PAM8 symbols with an entropy of 2.75 bit/symbol can be combined into PS-64QAM with an entropy of 5.5 bit/symbol (called PS-64QAM-5.5 here).

When considering overheads from CCDM and FEC, we transmit a total of V_1 64QAM symbols, which can only carry $2(U_1 + U_2)$ desired bits. Therefore, the actual transmission rate can be expressed as:

$$R_{actual} = \frac{2(U_1 + U_2)}{V_1} \quad (2)$$

In this way, the actual transmission rate of PS-64QAM-5.5 is only 4.2 bit/symbol. Our actual transmission rate is exactly consistent with the theoretical rate R for probabilistic shaping based on 64QAM constellations, which is obtained by

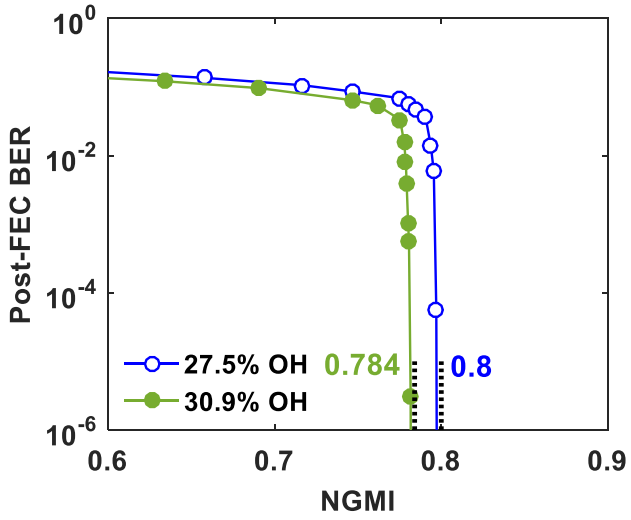

Fig. 3. Post-FEC BER as a function of NGMI with 27.5% and 30.9% SD-FEC overheads for PS-64QAM-5.5 and Hybrid-32/64QAM-5.5.

Equation 3 of Reference 12:

$$\mathrm{R} = H - (1 - r) \cdot m \tag{3}$$

where H is entropy (5.5 bit/symbol), r is FEC code rate (40/51), and m is 64QAM constellation bits per symbol (6 bit/symbol). In this way, the calculated theoretical transmission rate R is also 4.2 bit/symbol. Therefore, the net bit rate per channel can be calculated as 48 Gsymbol/s $\times$ 2 polarization $\times$ 4.2 bit/symbol/polarization = 403 Gbit/s.

Figure 3 shows the NGMI versus post-FEC BER after LDPC decoding when using LDPC with 40/51 and 55/72 code rates, corresponding to 27.5% and 30.9% overheads. As shown in Fig. 3, post-FEC error free performance can be achieved when the NGMI reaches up to 0.8 and 0.784 for the case with 27.5% and 30.9% overheads, respectively. In other words, 0.8 and 0.784-NGMI can be proven to be the SD-FEC threshold with 27.5% and 30.9% overheads, respectively. Here, the LDPC with 27.5% overhead is used on PS-64QAM-5.5 signal. While in order to get the same net bit rate, the LDPC with 30.9% overhead is used on regular-64QAM and hybrid-32/64QAM-5.5 signals.

III. Experimental Setup

The experimental setup and DSP principle of the generation and transmission of 8-channel 48-Gbaud WDM PS-64QAM (or hybrid-32/64QAM) signals are given by Fig. 4 and Fig. 5. In the transmitter DSP, hybrid-32/64QAM and PS-64QAM symbols, both with an entropy of 5.5 bit/symbol/polarization, were generated, respectively. For hybrid-32/64QAM, as shown in inset (a) of Fig. 5, 32QAM and 64QAM signals both account for a half of the time slots and appear alternately. As for PS-64QAM, we generated symbols with 5.5-bit/symbol/polarization entropy with designated Maxwell-Boltzmann distribution, and the probability distribution of generated PS-64QAM signals are illustrated in inset (b) of Fig. 5. After QAM-mapping, the generated PS-64QAM (or hybrid-32/64QAM) symbols were fed into a LUT pre-distortion and pre-equalization section based on a training sequence used for pre-processing training. Meanwhile, the raised cosine (RC) roll-off with a roll-off factor of 0.04 was applied, as shown in the transmitter DSP part of Fig. 5. The pre-equalization finite-impulse-response (FIR) with 1024 filter length was calculated according to the 21-tap coefficients of constant modulus algorithm (CMA) filter after convergence under the back-to-back (BtB) case, which is shown in Fig. 5-(c). The LUT-based pre-distortion shown in Fig. 5-(d) is carried out based on the training sequence after pre-equalization. The pattern dependent look-up table with 9-symbol memory is firstly generated by comparing the transmitted signals with the corresponding recovered ones. The average difference between the transmitted signals and the corresponding recovered ones for each pattern in the table index was calculated. Here around 35000 patterns were covered through several sets of 2^{16} length training sequences. The corresponding constellation of pre-distortion was generated lastly by the calculated average differences. Afterwards, the pre-processed signals were loaded into a digital-to-analog converter (DAC).

The transmitter-block consisted of a commercial DAC with 20-GHz analog bandwidth and 84-GSa/s sampling rate, a 100-kHz-linewidth external cavity laser (ECL), a 32-GHz-bandwidth I/Q modulator, two 65-GHz modulator drivers and a polarization multiplexer (Pol. MUX). For optical signal modulation, the light source at 1553.126-nm from the ECL was fed into the I/Q modulator driven by the pre-processed signals. After optical modulation, a Pol. MUX was utilized to realize polarization multiplexing. At the transmitter-side, 8-channel 50 GHz-WDM PM signals, which were divided into odd-channel group (Ch. 1, 3, 5 and 7) and even-channel group (Ch. 2, 4, 6 and 8), were combined by a polarization maintaining optical coupler (PM-OC) and launched into the recirculating ULAF loop with backward-pumped Raman amplifier, which consisted of several spans of 400-km TeraWave+ fiber with an average effective area of 125-μm^2, an attenuation coefficient of 0.182-dB/km and a chromatic dispersion coefficient of 20-ps/(nm·km) at 1550 nm. In the recirculating loop, a backward-pumped Raman amplifier with 20-dB ON-OFF gain was utilized to compensate for signal loss for each span. The average power of the Raman pumps is around 950-mW. What's more, we used an attenuator (ATT) to control the optical power and a WSS was used to flatten the gain slope of the band-pass filter.

At the receiver end, a tunable optical filter (TOF) with 3-dB bandwidth of 0.9 nm was used to select the desired sub-channel from the 8-channel WDM signals. In our experiment, the 4-th sub-channel is selected by the TOF. Then we implemented the polarization- and phase-diversity operation for the selected WDM signal and the 100-kHz-linewidth optical local oscillator (LO) using two polarization beam splitters (PBSs) and two 90° optical hybrids. Afterwards, the outputs of hybrids were fed into four balanced photodetectors (PDs), each with a bandwidth of 70-GHz. Finally, the digitization and sampling were realized by the digital oscilloscope (OSC) with 65-GHz bandwidth and 160-GSa/s sampling rate, which was followed by the offline DSP shown in Fig. 5. The offline DSP consisted of Butterworth digital low-pass filter, resampling, chromatic dispersion (CD) compensation, clock recovery, T/2 CMA, frequency offset estimation (FOE), carrier-phase-estimation (CPE) based on blind-phase-search (BPS), decision-directed least mean square (DD-LMS) equalization, decision and NGMI calculation.

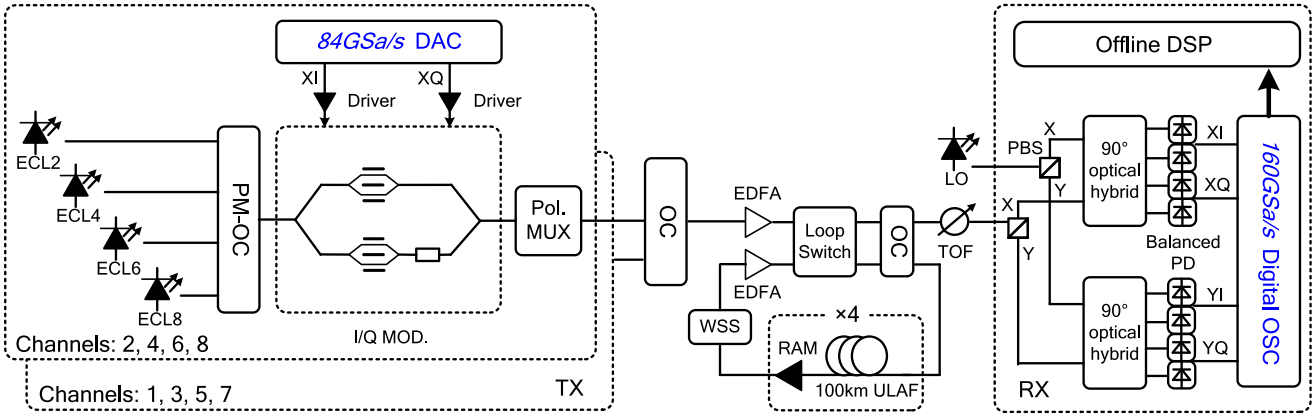

Fig. 4. Experimental setup of 8-channel WDM transmission over ULAF with Raman amplifier based on 48-Gbaud PM PS-64QAM or hybrid-32/64QAM.

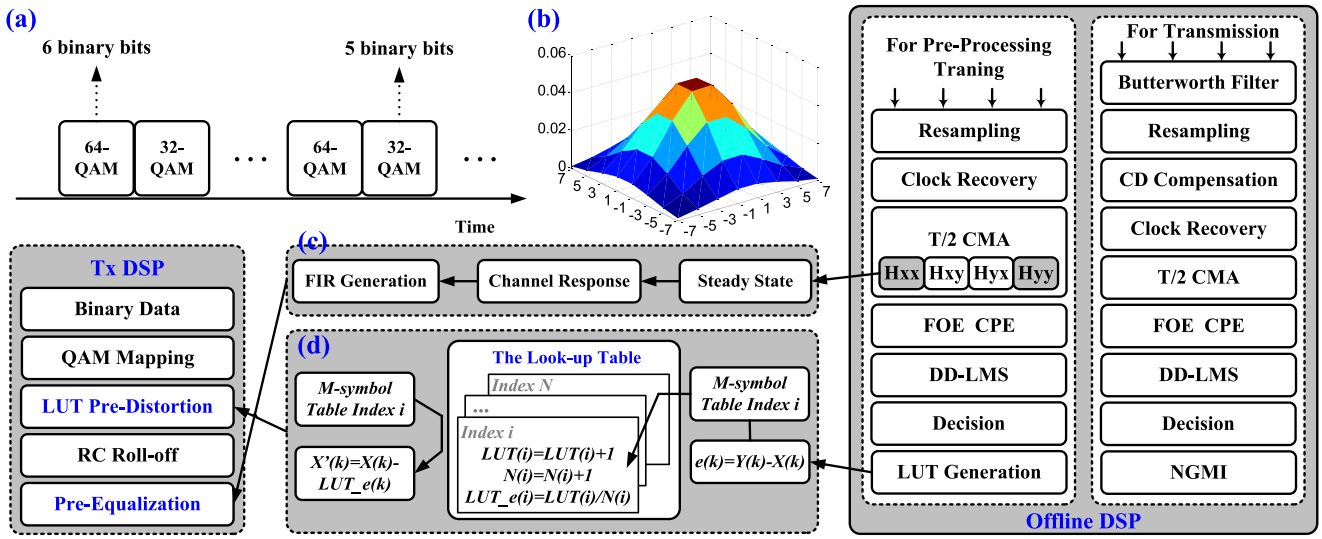

Fig. 5. Principle of Tx DSP, pre-processing and offline DSP after transmission. (a) Symbol mapping of hybrid-32/64QAM; (b) Probability distribution of PS-64QAM signals.

IV. Results

A. Results of Pre-Processing

In order to overcome the filtering effect from bandwidth limitation and component nonlinearity impairment, pre-equalization and LUT-based pre-distortion are carried out before the WDM transmission experiment. Received electrical spectra of 48-Gbaud hybrid-32/64QAM signals before and after pre-equalization are given in Fig. 6(a) and (b) respectively. As can be seen from Fig. 6(b), high frequency part is compensated. In addition, Fig. 7(a) and (b) show the LUT correction values of different pattern index and corresponding hybrid-32/64QAM symbols constellation in case of 9-symbol memory, respectively. As shown in Fig. 8, we can obtain around 3.6-dB OSNR gain when using pre-equalization compared with the case without pre-equalization. What is more, another 1.9-dB OSNR gain can be achieved by using the LUT based pre-distortion.

However, 48-G baud-rate is really close to 50-GHz WDM grid and serious crosstalk from adjacent WDM channels can be caused. In order to reduce the penalty caused by crosstalk between channels, RC roll-off with a roll-off factor of 0.04 is applied before WDM transmission, yielding around 0.6-dB OSNR penalty for all single-channel regular-32QAM, regular-64QAM and hybrid-32/64QAM signals, as shown in Fig. 9.

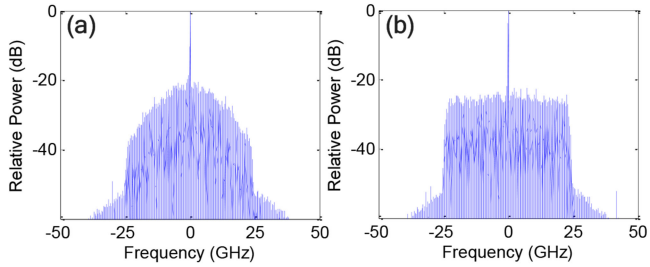

Fig. 6. Received electrical spectra of hybrid-32/64QAM signals (a) without and (b) with pre-equalization.

B. Comparison of OC and WSS in the WDM System

It is universally acknowledged that OC and WSS can be both used in WDM systems and crosstalk from adjacent WDM channels is the primary reason of penalty for both of them.

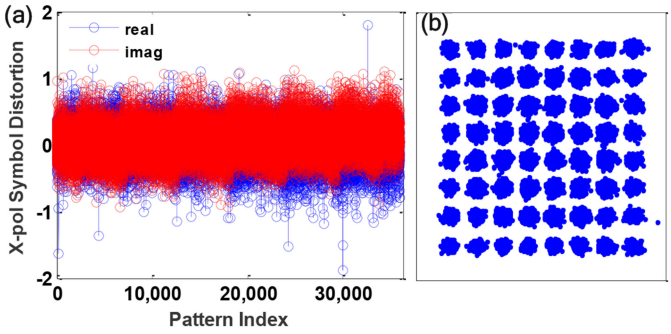

Fig. 7. (a) LUT correction values with 9-symbol memory; (b) corresponding constellation after LUT based pre-distortion.

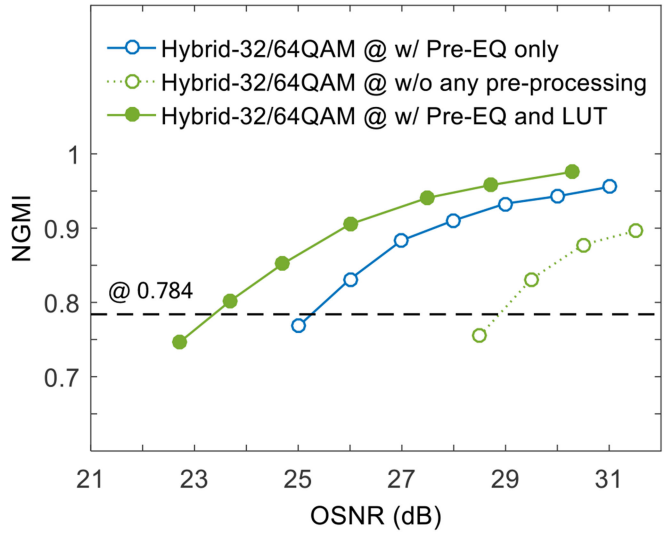

Fig. 8. NGMI results versus BtB OSNR for single-channel signals.

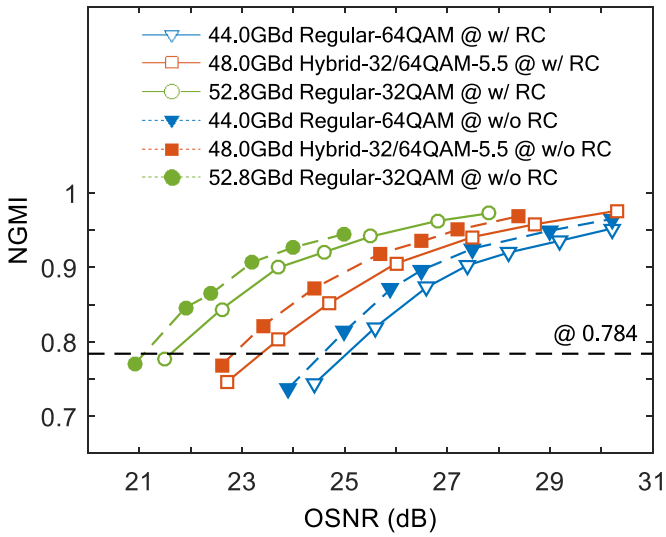

Fig. 9. BtB NGMI results versus BtB OSNR for single-channel regular-32QAM, regular-64QAM and hybrid-32/64QAM signals.

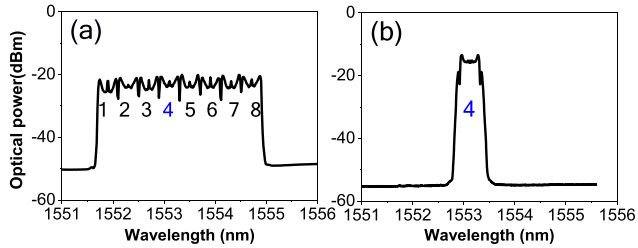

Fig. 10. Optical spectra of (a) 8-channel WDM hybrid-32/64QAM signals using OC and (b) selected channel-4 WDM signals.

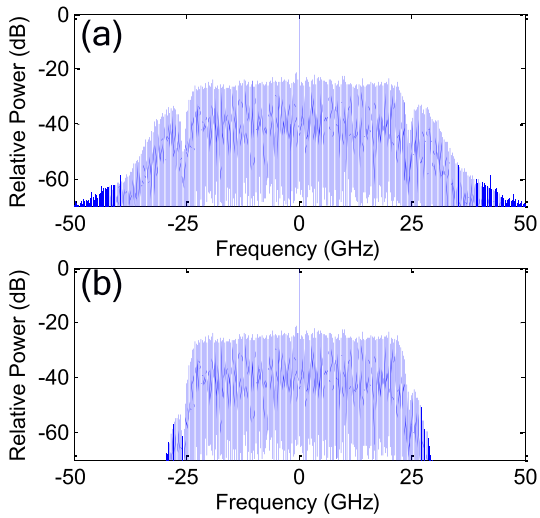

Fig. 11. Electrical spectra of selected channel-4 WDM hybrid-32/64QAM signals (a) before and (b) after low-pass filter.

Especially, we add a 15-th-order Butterworth digital low-pass filter with a passband below the ratio of baud-rate and sample rate before resampling in the offline DSP to minimize the impact of crosstalk from adjacent channels.

The optical spectra of eight-channel WDM hybrid-32/64QAM signals using OC is illustrated in Fig. 10-(a). Then the 4-th sub-channel of WDM hybrid-32/64QAM signals is selected by TOF and the optical spectra is shown in Fig. 10-(b). At the beginning of offline DSP, the electrical spectra of the selected channel-4 signal is given by Fig. 11-(a) and the electrical spectra of the signal processed by the 15-th-order Butterworth digital low-pass filter is shown in Fig. 11-(b). By utilizing low-pass filter, the WDM signals using OC (called modified OC in Fig. 12) can obtain around 0.6-dB OSNR gain compared with the case without low-pass filter, as shown in Fig. 12. Thus, the low-pass filter is used by default in our subsequent experiments.

It is illustrated in Fig. 13 that the WDM hybrid-QAM signals using OC incurs around 1-dB OSNR penalty compared with the single-channel case due to the crosstalk from adjacent channels. While the case using WSS can obtain around 2.5-dB penalty. The reason the WSS case incurs more penalty is that extra penalty can be added by filtering effect of WSS with the narrow passband. In order to overcome the filtering effect of WSS, the pre-equalization is carried out under WSS (called modified WSS in Fig. 13), which yields around 0.9-dB OSNR gain, but there is still around 0.7-dB OSNR gap between OC and WSS. Thus, the OC is selected in our following experiments.

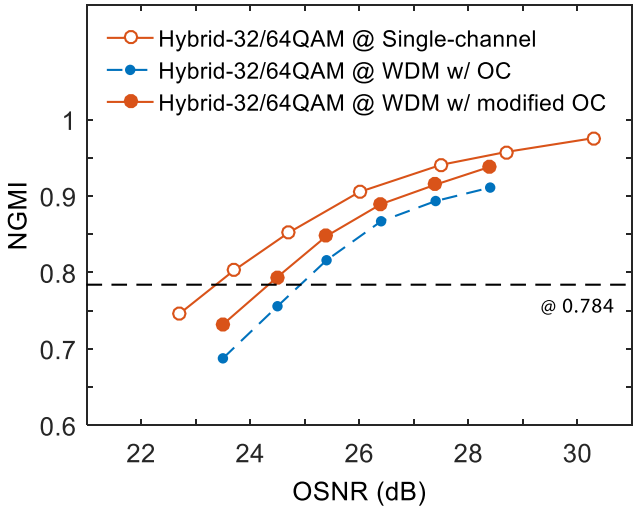

Fig. 12. NGMI results versus BtB OSNR for channel-4 WDM hybrid-32/64QAM signal using OC.

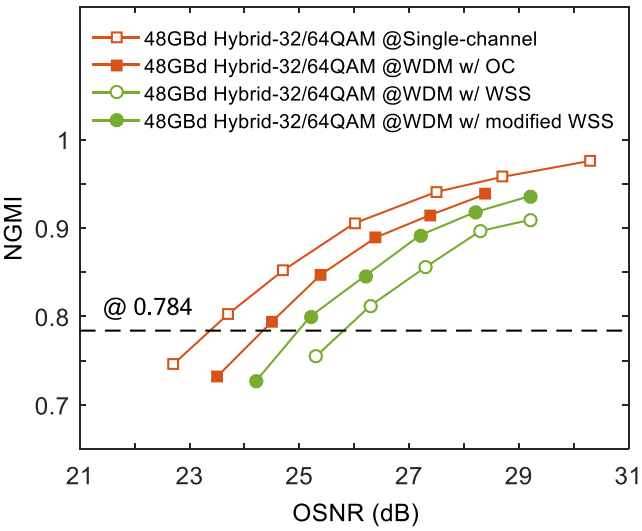

Fig. 13. NGMI versus BtB OSNR for hybrid-32/64QAM signal.

C. Choice of Hybrid Ratio for Hybrid-32/64QAM

Figs. 14-(a) and 14-(b) show single-channel and WDM signals using several different modulation formats respectively. As we know, high-level QAM like 64QAM is needed to meet the requirement of 400-Gbit/s bit-rate per channel. The SD-FEC threshold with 30.9% overhead requires 44-Gbaud rate for regular-64QAM. However, higher OSNR requirement limits the transmission distance for 64QAM. Compared with regular-64QAM, single channel 52.8-Gbaud 32QAM can obtain around 3.5-dB OSNR gain as shown in Fig. 14(a), but 52.8G baud-rate is not available for 50-GHz WDM grid. By chance, the gap between regular-32QAM and regular-64QAM can be filled smoothly by hybrid-32/64QAM.

For the single-channel case, the hybrid-32/64QAM signals can obtain a better OSNR sensitivity when the entropy is closer to 5-bit/symbol/polarization. However, lower entropy means a higher baud-rate, which may introduce more penalty caused by crosstalk from adjacent WDM channels. In order to choose

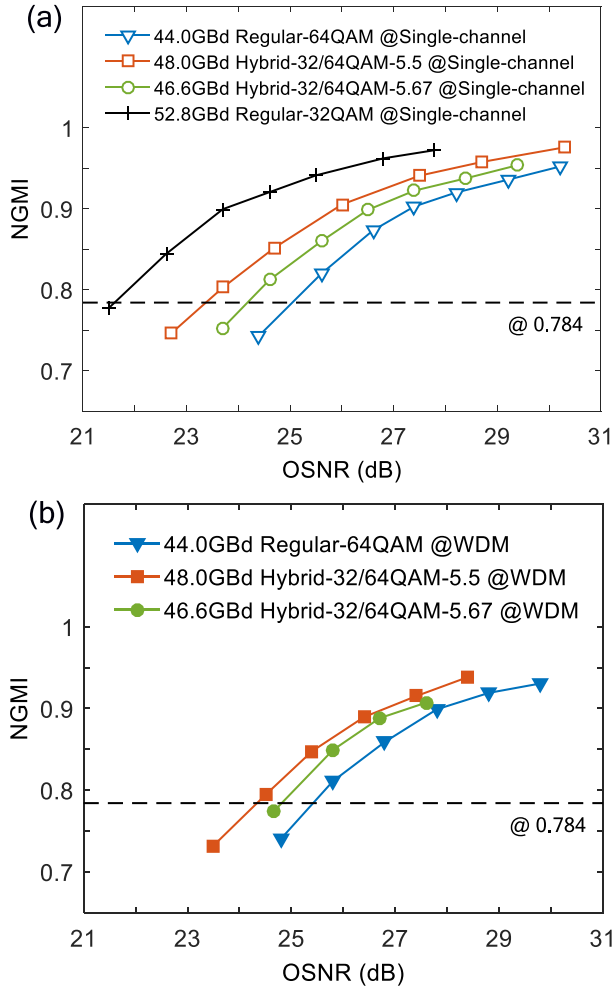

Fig. 14. NGMI results versus BtB OSNR for (a) single-channel and (b) channel-4 WDM signals.

an optimal hybrid ratio (entropy) for hybrid-32/64QAM, we carry out single-channel and WDM experiments at BtB case based on the hybrid ratio of 1:1 (5.5-bit/symbol) and 1:2 (5.67-bit/symbol), respectively.

For the single-channel case, as shown in Fig. 14 (a), hybrid-32/64QAM signals with an entropy of 5.67-bit/symbol/polarization obtains around 0.9-dB OSNR gain compared with regular-64QAM, while hybrid-32/64QAM-5.5 outperforms hybrid-32/64QAM-5.67 by around 0.8-dB gain. As for WDM signals, as illustrated in Fig. 14 (b), regular-64QAM signals incur the least crosstalk penalty, which is only around 0.2-dB, compared with the single-channel case. WDM hybrid-32/64QAM-5.5 signals obtain about 0.9-dB OSNR penalty compared with the single-channel case, which is the most among all three formats of regular-64QAM, hybrid-32/64QAM-5.5, and hybrid-32/64QAM-5.67. However, thanks to its more advantage on the single-channel sensitivity, WDM hybrid-32/64QAM-5.5 still performs the best among all three formats and obtains around 0.5-dB and 1.1-dB OSNR gain compared with hybrid-32/64QAM-5.67 and regular-64QAM, respectively. As a result, the hybrid-32/64QAM with a hybrid ratio of 1:1 (5.5-bit/symbol) is selected as the optimal

TABLE I
EXPERIMENTAL RESULTS OF WDM REGULAR-64QAM, HYBRID-32/64QAM AND PS-64QAM

Modulation formats	Baud rate per channel	SD-FEC overhead	Net bit rate per channel	SE	OSNR sensitivity	SSMF reach	ULAF reach
Regular-64QAM	44 Gbaud	30.9%	403.3 Gbit/s	8.06 b/s/Hz	25.3 dB	630 km	2,000 km
Hybrid-32/64QAM-5.5	48 Gbaud	30.9%	403.3 Gbit/s	8.06 b/s/Hz	24.2 dB	720 km	2,400 km
PS-64QAM-5.5	48 Gbaud	27.5%	403.7 Gbit/s	8.07 b/s/Hz	22.7 dB	990 km	3,600 km

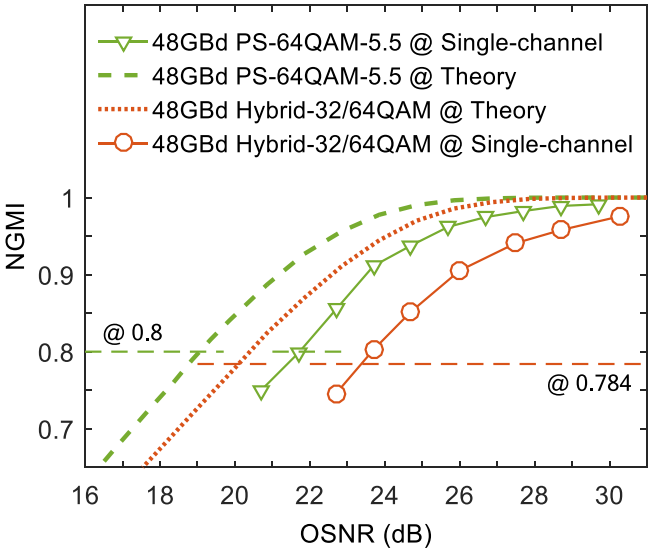

Fig. 15. Theoretical and experimental NGMI results versus BtB OSNR for single-channel hybrid-32/64QAM and PS-64QAM signals.

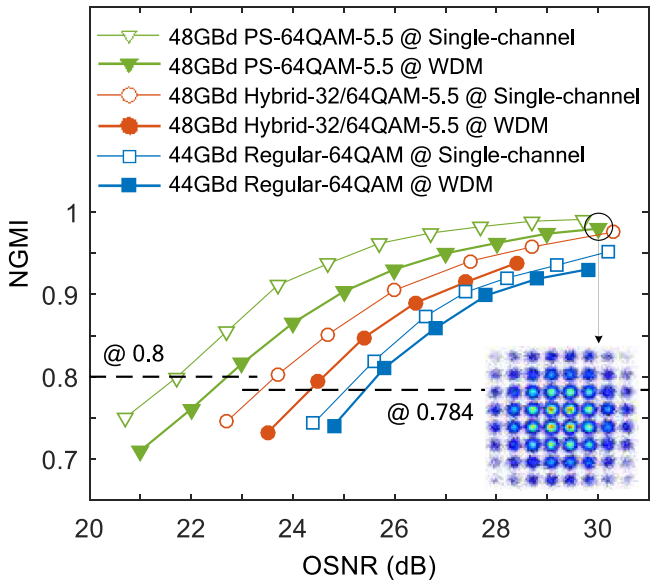

Fig. 16. NGMI results versus BtB OSNR for regular-64QAM, hybrid-32/64QAM and PS-64QAM signals.

hybrid-32/64QAM modulation formats in our experiment, not only satisfying the requirement of 50-GHz WDM, but also obtaining better OSNR sensitivity.

D. Comparison of PS-64QAM and Hybrid-32/64QAM

Firstly, the theoretical and experimental NGMI results versus BtB OSNR for single-channel hybrid-32/64QAM and PS-64QAM signals with an entropy of 5.5-bit/symbol/polarization are illustrated in Fig. 15. PS-64QAM and hybrid-32/64QAM signals incur around 2.8-dB and 3.4-dB OSNR penalty compared with theory results, respectively. PS-64QAM signals incur lower penalty because the probability distribution of outermost constellation points is lower and the performance in overcoming nonlinearity impairment is better for PS-64QAM compared with hybrid-32/64QAM.

The WDM experiment results of measured NGMI versus BtB OSNR for regular-64QAM, hybrid-32/64QAM and PS-64QAM are given in Fig. 16. There is around 0.9-dB OSNR penalty for both 48-Gbaud WDM PM hybrid-32/64QAM-5.5 and PS-64QAM-5.5 signals compared with single-channel case. The required OSNR for WDM PS-64QAM signals (528-Gbit/s line rate and 403-Gbit/s net bit rate) at the SD-FEC threshold with 27.5% overhead of 0.8 NGMI is around 22.7-dB, which obtains around 2.6-dB OSNR gain compared with 44-Gbaud regular-64QAM (528-Gbit/s line rate and 403-Gbit/s net bit rate) at 30.9% SD-FEC threshold of 0.784 NGMI. For hybrid-32/64QAM with the same baud-rate and bit-rate as PS-64QAM, however, only 1.1-dB OSNR gain can be obtained compared with regular-64QAM.

Afterwards, we carry out an eight-channel 50-GHz WDM transmission experiment over several spans of 90-km EDFA-amplified standard single-mode fiber (SSMF) and several spans of 400-km ULAF (TeraWave-SLA+ fiber, 122-μm^2 average effective area) with backward-pumped Raman amplifier, respectively. The transmission results over SSMF and ULAF of the 4-th WDM sub-channel is illustrated in Fig. 17 and Fig. 18-(a), respectively. It can be demonstrated that the SSMF transmission of WDM PM PS-64QAM signals with a net bit rate of 403-Gbit/s over up to 990-km can be fulfilled with measured NGMI above the 27.5% SD-FEC threshold of 0.8 NGMI, leading to 37.5% SSFM transmission distance improvement compared with hybrid-32/64QAM (720-km). Simultaneously, 403-Gbit/s WDM PS-64QAM signals can be transmitted over 3,600-km Raman-amplified ULAF, obtaining apparent transmission distance improvement (more than 250%) compared with EDFA-amplified SSMF. Moreover, WDM PS-64QAM signals can obtain 80% ULAF transmission distance improvement compared with regular-64QAM (2,000-km), while transmission over 2,400-km ULAF can be realized based on WDM hybrid-32/64QAM, leading to only 20% reach improvement compared with regular-64QAM. In other words, PS-64QAM can outperform hybrid-32/64QAM by 50% reach improvement in the aforementioned 50-GHz WDM system with a bit rate

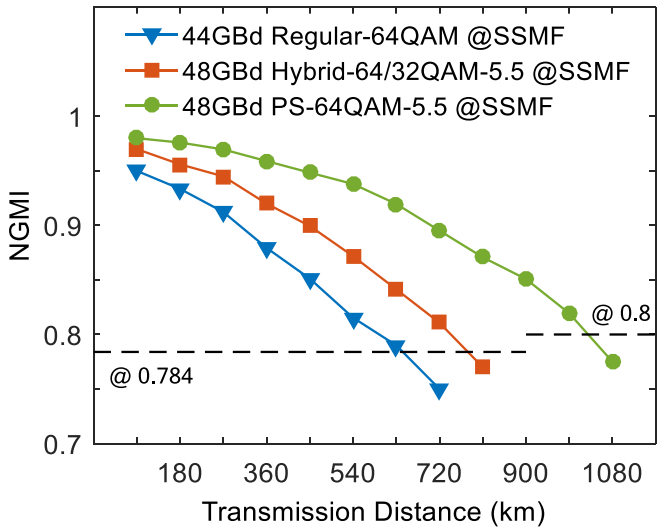

Fig. 17. NGMI versus SSMF transmission distance for channel-4 WDM regular-64QAM, hybrid-32/64QAM and PS-64QAM signals.

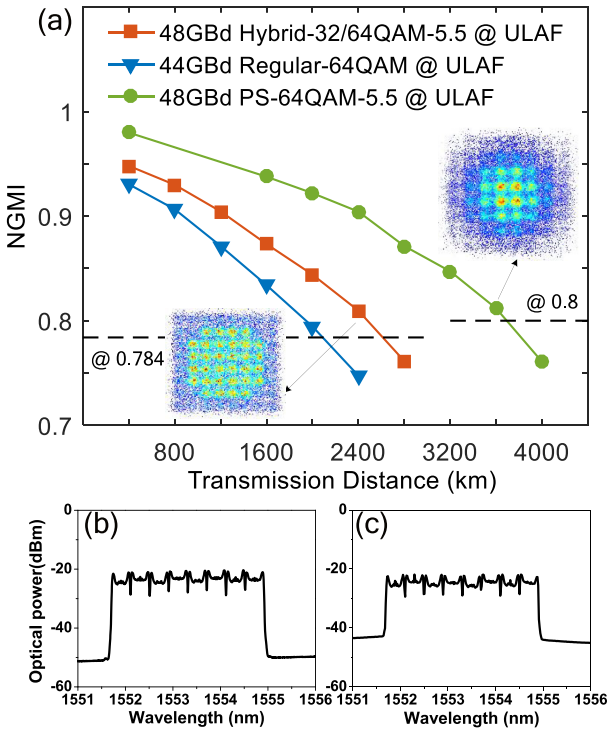

Fig. 18. (a) NGMI versus ULAF transmission distance for channel-4 WDM regular-64QAM, hybrid-32/64QAM and PS-64QAM signals; optical spectra of 8-channel WDM PS-64QAM signals (b) before and (c) after 3600-km ULAF transmission.

of 400G per channel. In addition, we have summarized the above experimental results in Table I. Besides, Figs. 18-(b) and 18-(c) offer the optical spectra of 8-channel WDM PS-64QAM signals before and after 3,600-km ULAF transmission, respectively.

What is more, the NGMI results versus optical input power for the 4-th sub-channel of WDM PS-64QAM signals after 3,600-km ULAF transmission is illustrated in Fig. 19 and the optimal input optical power per channel is about 0.5-dBm. When

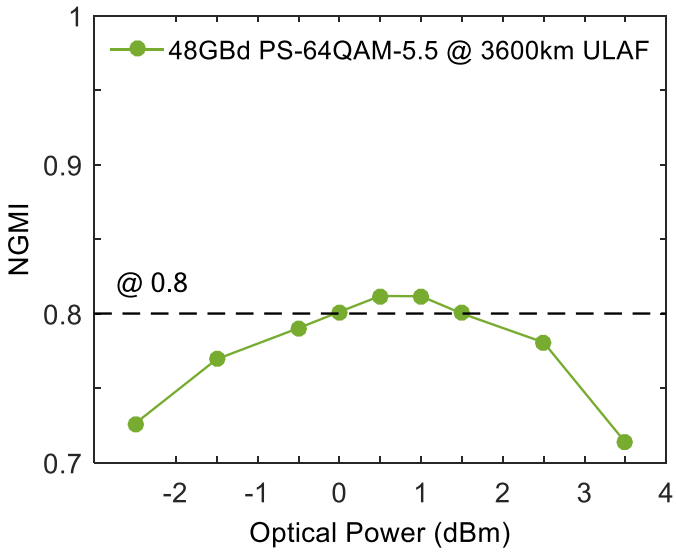

Fig. 19. NGMI versus optical power for channe-4 WDM PS-64QAM signals after 3,600-km ULAF transmission.

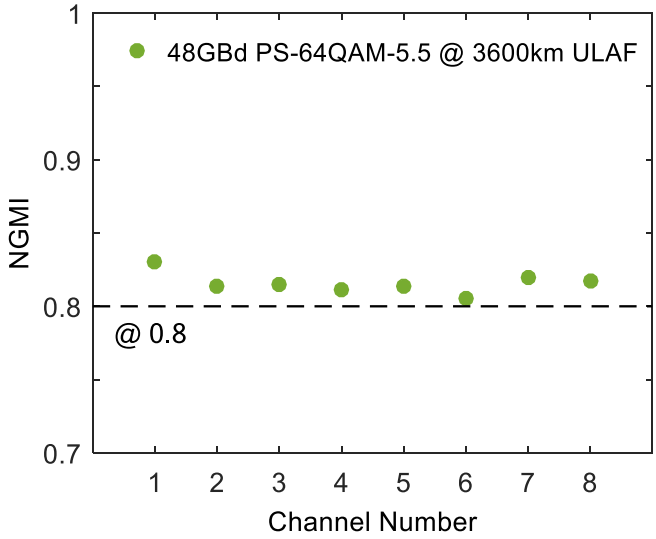

Fig. 20. NGMI results of all 8 channels for PS-64QAM signals after 3,600-km ULAF transmission.

optical power is too low, the OSNR is not enough for reliable transmission, while if the power is too high, the photodiode will be saturated. The reliable input optical power range is around 0-dB∼1.5-dB for 3,600-km WDM PS-64QAM transmission. In addition, Fig. 20 shows that the measured NGMI values of all eight WDM channels after 3,600-km ULAF transmission are all above 0.8, which is 27.5% SD-FEC threshold. It can be concluded that the eight-channel WDM transmission with a net bit rate of 403-Gbit/s over 3,600-km Raman-amplified ULAF based on PM PS-64QAM can be fulfilled.

V. Conclusion

The PS technology, pre-equalization, LUT-based pre-distortion and ULAF with Raman amplification have allowed us to experimentally realize the eight-channel 50-GHz WDM coherent transmission over 3,600-km ULAF based on 403-Gbit/s

net-bit-rate PM PS-64QAM at 48-Gbaud when considering the 27.5% SD-FEC threshold of 0.8 NGMI, which obtains 80% transmission distance improvement compared with the regular-64QAM and outperforms hybrid-32/64QAM by 50% reach improvement in the 400G per channel 50-GHz WDM system. The application of DM and Maxwell-Boltzmann distribution makes PS-QAM more power-efficient than hybrid-QAM and other modulation formats for high-speed and long-reach coherent optical transmission.

We have confirmed that pre-processing, namely pre-equalization and LUT-based pre-distortion, can effectively overcome the filtering effect from bandwidth limitation and component nonlinearity impairment. By carrying out pre-equalization and LUT, we can obtain around 5.5-dB OSNR gain for single-channel hybrid-32/64QAM signals.

It has been concluded that the combination of RC roll-off pre-processing, OC and low-pass digital filter during DSP can offer a suitable way for WDM transmission. Moreover, we have compared OC with WSS in 50-GHz WDM transmission for 48-Gbaud hybrid-32/64QAM signals. The utilization of OC incurs only 1-dB penalty compared with the single-channel case, which is 0.7-dB lower than WSS. Meanwhile, using the 15-th order Butterworth low-pass digital filter before resampling during DSP, we can obtain around 0.6-dB OSNR gain for 48-Gbaud 50-GHz WDM hybrid-32/64QAM signals with OC.

Besides, as a sleek transition between regular-32QAM and regular-64QAM, hybrid-32/64QAM can yield a better compromise between spectral efficiency and OSNR sensitivity than regular-32QAM and regular-64QAM. The hybrid-32/64QAM with an entropy of 5.5-bit/symbol/polarization can be a reliable hybrid scheme for 50-GHz WDM with a bit rate of 400 Gbit/s per channel, which can obtain around 0.5-dB and 1.1-dB sensitivity gain compared with regular-64QAM and hybrid-32/64QAM-5.67 at WDM case, respectively.

We have also compared PS-64QAM with hybrid-32/64QAM signals with an entropy of 5.5-bit/symbol/polarization in 48-Gbaud 50-GHz WDM transmission. It can be concluded that PS-64QAM signals can obtain around 1.5-dB WDM sensitivity gain and around 50% ULAF transmission distance improvement compared with the hybrid-32/64QAM. In addition, the application of Raman-amplified ULAF offers apparent transmission distance improvement (more than 250%) compared with EDFA-amplified SSMF.

REFERENCES

[1] J. Yu *et al.*, "8 × 506-Gb/s 16QAM WDM signal coherent transmission over 6000-km enabled by PS and HB-CDM," in *Proc. Opt. Fiber Commun. Conf. Expo.*, 2018, Paper M2C.3.

[2] J. Yu *et al.*, "8 × 528-Gb/s PS-64QAM transmission over 3000 km in a terrestrial system with an amplifier span of 100 km," in *Proc. Eur. Conf. Opt. Commun.*, 2018, Paper M2C.3.

[3] J. H. Ke, Y. Gao, and J. C. Cartledge, "400 Gbit/s single-carrier and 1 Tbit/s three-carrier super channel signals using dual polarization 16-QAM with look-up table correction and optical pulse shaping," *Opt. Express*, vol. 22, no 1, pp. 71–83, 2014.

[4] Y. Zhu *et al.*, "Spectrally-efficient single-carrier 400G transmission enabled by probabilistic shaping," in *Proc. Opt. Fiber Commun. Conf. Expo.*, 2017, Paper M3C.1.

[5] G. Raybon *et al.*, "Single-carrier 400 G interface and 10-channel WDM transmission over 4800 km using all-ETDM 107-Gbaud PDMQPSK," in *Proc. Opt. Fiber Commun. Conf. Expo.*, 2013, Paper PDP5A.5.

[6] X. Zhou *et al.*, "High spectral efficiency 400 Gb/s transmission using PDM time-domain hybrid 32–64 QAM and training-assisted carrier recovery," *J. Lightw. Technol.*, vol. 31, no. 7, pp. 999–1005, Apr. 2013.

[7] X. Zhou *et al.*, "4000 km transmission of 50 GHz spaced 10 × 494.85 Gb/s hybrid 32–64 QAM using cascaded equalization and training-assisted phase recovery," in *Proc. Opt. Fiber Commun. Conf. Expo./Nat. Fiber Opt. Eng. Conf.*, 2012, Paper PDP5C. 6.

[8] P. Schulte and G. Böcherer, "Constant composition distribution matching," *IEEE Trans. Inf. Theory*, vol. 62, no. 1, pp. 430–434, Jan. 2016.

[9] L. Schmalen *et al.*, "Probabilistic constellation shaping: Challenges and opportunities for forward error correction," in *Proc. Opt. Fiber Commun. Conf. Expo.*, 2018, Paper M3C.1.

[10] T. Fehenberger, D. Lavery, R. Maher, A. Alvarado, P. Bayvel, and N. Hanik, "Sensitivity gains by mismatched probabilistic shaping for optical communication systems," *IEEE Photon. Technol. Lett.*, vol. 28, no. 7, pp. 786–789, Apr. 2016.

[11] F. R. Kschischang and S. Pasupathy, "Optimal nonuniform signaling for Gaussian channels," *IEEE Trans. Inf. Theory*, vol. 39, no. 3, pp. 913–929, May 1993.

[12] G. Böcherer, F. Steiner, and P. Schulte, "Bandwidth efficient and rate-matched low-density parity-check coded modulation," *IEEE Trans. Commun.*, vol. 63, no. 12, pp. 4651–4665, Dec. 2015.

[13] T. Fehenberger, A. Alvarado, G. Böcherer, and N. Hanik, "On probabilistic shaping of quadrature amplitude modulation for the nonlinear fiber channel," *J. Lightw. Technol.*, vol. 34, no. 21, pp. 5063–5073, Nov. 2016.

[14] J. Cho *et al.*, "Trans-Atlantic field trial using probabilistically shaped 64-QAM at high spectral efficiencies and single-carrier real-time 250-Gb/s 16-QAM," in *Proc. Opt. Fiber Commun. Conf. Expo.*, 2017, Paper Th5B.3.

[15] J. Zhang *et al.*, "WDM transmission of 16-channel single-carrier 128-GBaud PDM-16QAM signals with 6.06 b/s/Hz SE," in *Proc. Opt. Fiber Commun. Conf. Expo.*, 2017, Paper Tu2E.5.

[16] J. Cho *et al.*, "Normalized generalized mutual information as a forward error correction threshold for probabilistically shaped QAM," in *Proc. Eur. Conf. Opt. Commun.*, 2017, Paper M.2.D.2.

[17] R. Maher *et al.*, "Constellation shaped 66 GBd DP-1024QAM transceiver with 400 km transmission over standard SMF," in *Proc. Eur. Conf. Opt. Commun.*, 2017, Paper Th.PDP.B.2.

[18] J. Zhang, J. Yu, and H. C. Chien, "High symbol rate signal generation and detection with linear and nonlinear signal processing," *J. Lightw. Technol.*, vol. 36, no. 2, pp. 408–415, Jan. 2018.

[19] J. Zhang, J. Yu, and H. C. Chien, "Time-domain digital pre-equalization for band-limited signals based on receiver-side adaptive equalizers," *Opt. Express*, vol. 22, no. 17, pp. 20515–20529, 2014.

[20] Z. Jia *et al.*, "Experimental demonstration of PDM-32QAM single-carrier 400G over 1200-km transmission enabled by training-assisted pre-equalization and look-up table," in *Proc. Opt. Fiber Commun. Conf. Expo.*, 2016, Paper Tu3A.4.

[21] A. Napoli, M. M. Mezghanni, S. Calabrò, R. Palmer, G. Saathoff, and B. Spinnler, "Digital pre-distortion techniques for finite extinction ratio IQ Mach–Zehnder modulators," *J. Lightw. Technol.*, vol. 35, no. 19, pp. 4289–4296, Oct. 2017.

[22] P. W. Berenguer *et al.*, "Nonlinear digital pre-distortion of transmitter components," *J. Lightw. Technol.*, vol. 34, no. 8, pp. 1739–1745, Apr. 2016.

[23] D. Rafique, A. Napoli, S. Calabro, and B. Spinnler, "Digital pre-emphasis in optical communication systems: On the DAC requirements for terabit transmission applications," *J. Lightw. Technol.*, vol. 32, no. 19, pp. 3247–3256, Oct. 2014.

[24] X. Zhou *et al.*, "64-Tb/s, 8 b/s/ Hz, PDM-36QAM transmission over 320 km using both pre- and post-transmission digital signal processing," *J. Lightw. Technol.*, vol. 29, no. 4, pp. 571–577, Feb. 2011.

[25] J. Zhang, J. Yu, and H. C. Chien, "Single-carrier 400G based on 84-Gbaud PDM-8QAM transmission over 2125 km SSMF enhanced by preequalization, LUT and DBP," in *Proc. Opt. Fiber Commun. Conf. Expo.*, 2017, Paper Tu2E.2.

[26] H. C. Chien, Z. Jia, and J. Yu, "256-Gb/s single-carrier PM-256QAM implementation using coordinated DD-LMS and CMA equalization," in *Proc. Eur. Conf. Opt. Commun.*, 2015, Paper Mo.3.3.2.